# Source Localization of Simulated Electroencephalogram of Virtual Epileptic Patient to Investigate Clinically Feasible Montages

**Zoe Herrick, Ping Li, and Anirban Dutta**

**Abstract** Electroencephalogram (EEG) source localization is used to estimate regions of ictal onset in epilepsy patients with temporal lobe epilepsy. Localization of EEG data struggles to achieve high spatial resolution, especially in deep brain regions, and is difficult to validate. In this paper we generate simulated EEG data using a spatiotemporally realistic generative brain network model (BNM) based on patient structural and functional data, created with The Virtual Brain (TVB) platform, to qualitatively assess head model approaches, distributed source inverse methods and clinically feasible electrode montages. We find that sLORETA is highly sensitive to head model errors, where dSPM is robust and wMNE displays some sensitivity. Additionally, increased electrode density over regions of interest provides a clinically feasible means to improve localization accuracy of a sparse montage. Finally, TVB platform can be utilized to model patient anatomy and physiology where resultant simulated EEG can be source localized for personalized neurological care.

## 1  Introduction

Focal epilepsy, characterized by seizures which originate in one region of the brain, accounts for 60% of the ~2.3 million adults and more than 450,000 adolescents who live with epilepsy in the US alone [1]. Of those with focal epilepsy, 60% have temporal lobe epilepsy (TLE), which is subdivided into two major categories. Neocortical or lateral TLE involves outer regions of the temporal lobe. Mesial TLE originates in medial structures such as the hippocampus and comprises 80% of those with TLE [2]. Determining seizure onset location in these cases is difficult due to depth within the brain. Invasive stereoelectroencephalography (sEEG) depth electrodes are often used for a more precise estimate. Proximity to regions vital for language

Z. Herrick · P. Li · A. Dutta (✉)
University at Buffalo SUNY, Buffalo, USA
e-mail: anirband@buffalo.edu

Z. Herrick
e-mail: zoeherri@buffalo.edu

processing and memory makes accurate identification of the onset region imperative for a successful post-surgical outcome. The National Institute of Neurological Disorders and Stroke (NINDS) has targeted some research toward developing methods for accurately mapping relevant areas of the brain in preoperative planning. They do so with the use of imaging tech in an effort to minimize language deficits that can occur. Research has shown that high density EEG localization is capable of achieving high accuracy, however this is often not feasible in clinical settings due to the expense of equipment. This paper qualitatively assesses head model approaches, distributed source inverse methods and clinically feasible electrode montages through the lens of spatiotemporally realistic simulated EEG data produced by a generative BNM.

## 2   Methods

### 2.1   The Virtual Brain

TVB is openly available and simulates brain activity with a generative BNM. Brain regions, or nodes, are heterogeneously modeled as discrete neural mass models with a connectivity matrix modeled after patient white matter tracts governing strength and time delay of network connections [3]. The Epileptor model [4] was chosen to govern all nodes with variable epileptogenicity, $x_0$, assigned to each node. Three model configurations were created, identical except for the $x_0$ parameter, and named according to their network role; Epileptogenic zones, Propagation zones, and Other Nodes were assigned $x_0$ values $-1.6$, $-1.8$, and $-2.4$ respectively. Increased negativity indicates stability with bifurcation of stable and epileptogenic behavior marked by critical value $x_{0c} = -2.04$. The amygdala, hippocampal cortex, and parahippocampal cortex in the right hemisphere (radiological convention in MNI atlas space) were assigned as Epileptogenic zones where the model could autonomously generate seizures. Propagation zones were the right ventral temporal cortex and superior temporal cortex, where seizure activity could spread but not originate. All other nodes were assigned as such and thus modeled as healthy tissue unaffected by epileptic activity. Simulated brain activity was mapped to 63 simulated EEG electrodes on the model scalp surface with a forward model to produce EEG data.

### 2.2   Brainstorm

Brainstorm ICBM 152_2019 anatomy template was selected as the protocol default anatomy for all subjects. Using the OpenMEEG software [5], BEM surfaces were generated via the Brainstorm approach, not Field Trip, for computational efficiency and warped using the simulated electrode locations. For each of three head models,

one surface and two volume, five montages were applied ranging from sparse 10–20 to the full montage of 63 electrodes. Assuming unconstrained sources, weighted minimum norm (wMNE), dynamic statistical parametric mapping (dSPM), and standardized low resolution electromagnetic tomography (sLORETA) inverse methods were applied to each head model as kernels to optimize hard drive space and computation time. A custom color bar scale was applied for each inverse method due to their distinct mathematical approaches producing varied units. Scales had a minimum value of 0 and maximum value of 0.15, 2.00e+9, and 7.00 for wMNE, dSPM, and sLORETA respectively.

## 3   Results

Of the 3 short seizures simulated, the first was selected for analysis after clinical assessment deemed it most realistic. TVB simulation data revealed seizure onset was in the right hippocampus (radiological convention in MNI atlas space). dSPM (Fig. 1a) failed to lateralize, producing bitemporal localization but displayed no mis-localization of the medial source on lateral surfaces. Activation was near ground truth, falling superiorly and posteriorly to the hippocampi. wMNE (Fig. 1b) mis-localized heavily to the lateral cortex surface. Strongest activation was seen on the anterior left temporal lobe (neurological convention), roughly superficial to the appropriate medial region in the expected hemisphere. sLORETA activation (Fig. 1c) was highly disperse and trended from the ventral temporal region towards the parietal lobe, correlating strongly with the region of greatest head model warping. Results were split across hemispheres but estimated activation was greater on the left with strongest activation on the inferior ventral left temporal lobe.

   Montage impact is best observed in sLORETA results (Fig. 2) by the parietal shift. A similar trend is observed in activation strength of dSPM results, which represents model confidence. The temporal montage (Fig. 2c), comprised of the sparse 10–20 montage and 5 additional electrodes at each temporal lobe, displayed localization results comparable to those achieved with the full montage (Fig. 2a). Application of one additional electrode in each temporal region (Fig. 2d) marginally improved localization beyond the 10–20 montage results (Fig. 2e). Selectively increasing density in temporal ROIs (Fig. 2c) significantly improved localization results of the sparse montage while an increase in general density (Fig. 2b) beyond the temporal montage did not show significant improvement, supporting selectively dense sparse montages.

## 4   Conclusion

Simulated epileptic EEG data generated in TVB can be used to assess distributed source localization methods on a spatiotemporal scale. Assessment of localization
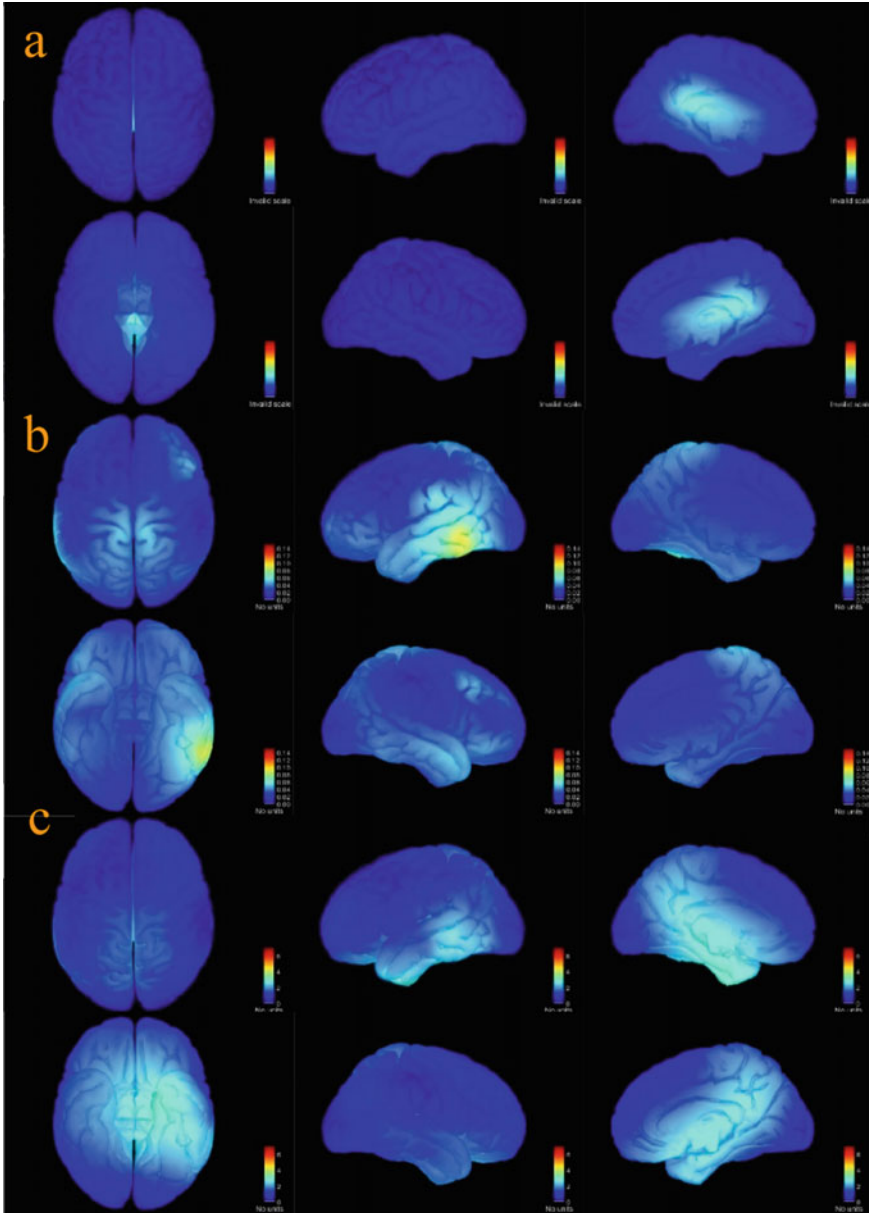
**Fig. 1** Comparison of localization estimations of distributed source inverse methods at seizure 1 onset on surface head model. For dSPM (**a**), wMNE (**b**) and sLORETA (**c**), 6 images display various cortical surfaces. Moving right from upper left, images depict top, left lateral, left medial, bottom, right lateral and right medial views. In top and bottom cases, anterior points up. Red indicates strongest activation on each color scale
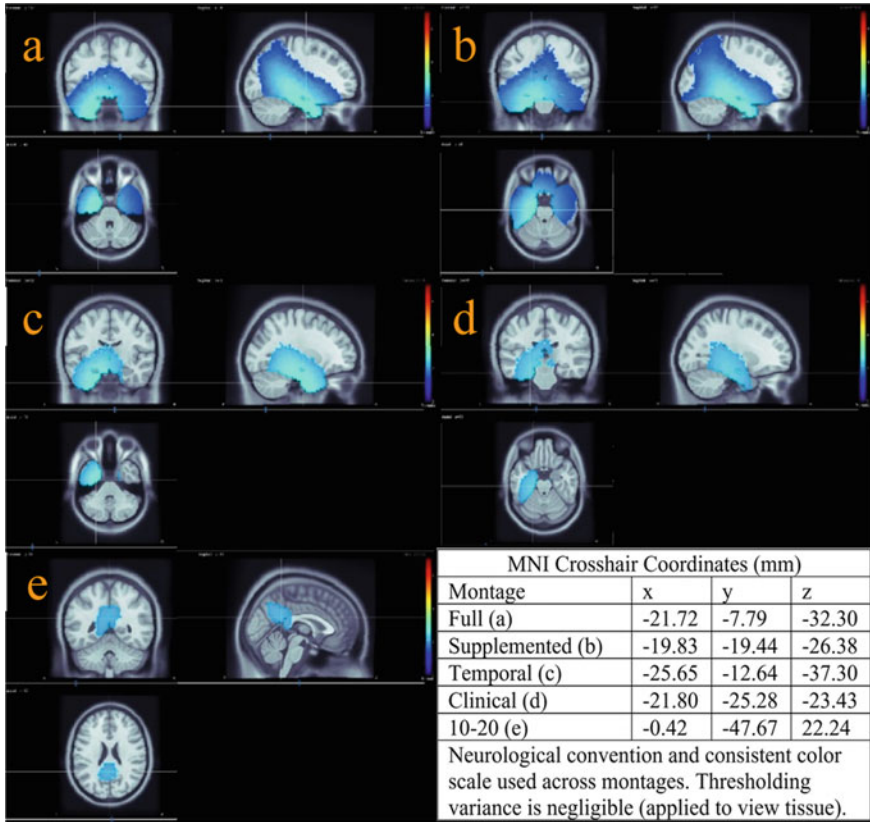
| MNI Crosshair Coordinates (mm) | | | |
|---|---|---|---|
| Montage | x | y | z |
| Full (a) | -21.72 | -7.79 | -32.30 |
| Supplemented (b) | -19.83 | -19.44 | -26.38 |
| Temporal (c) | -25.65 | -12.64 | -37.30 |
| Clinical (d) | -21.80 | -25.28 | -23.43 |
| 10-20 (e) | -0.42 | -47.67 | 22.24 |
| Neurological convention and consistent color scale used across montages. Thresholding variance is negligible (applied to view tissue). | | | |

**Fig. 2** Comparison of sLORETA localization results on adaptive grid volume head model across 5 montages. Table of crosshair locations denotes montages. As montage sparsity increases, estimated activation shifts into the parietal lobe and decreases in strength. Color bar scale is consistent across montages. Thresholding varies only for visualization of underlying tissue. Location and intensity of highest color bar value region is the focus

results achieved with this data elucidates the potential for clinically feasible selectively dense montages to optimize localization in a clinical setting. Personalized neurological care for TLE patients is possible with this approach. A bottleneck exists in generation of the simulated data but can be overcome with an individual trained in TVB collaborating with clinicians.

# References

1. O. o. C. a. P. L. NINDS, *Epilepsy: Hope Through Research.* NIH. https://www.ninds.nih.gov/Disorders/Patient-Caregiver-Education/Hope-Through-Research/Epilepsies-and-Seizures-Hope-Through. Accessed 7/1/2020
2. H. Klein, C. Joshi, *Temporal Lobe Epilepsy (TLE).* Epilepsy Foundation of America. https://www.epilepsy.com/learn/types-epilepsy-syndromes/temporal-lobe-epilepsy-aka-tle. Accessed 7/1/2020
3. V.K. Jirsa et al., The virtual epileptic patient: individualized whole-brain models of epilepsy spread. Neuroimage **145**, 377–388 (2017). https://doi.org/10.1016/j.neuroimage.2016.04.049
4. V.K. Jirsa, W.C. Stacey, P.P. Quilichini, A.I. Ivanov, C. Bernard, On the nature of seizure dynamics, (in eng). Brain **137**(Pt 8), 2210–2230 (2014). https://doi.org/10.1093/brain/awu133
5. A. Gramfort, T. Papadopoulo, E. Olivi, M. Clerc, OpenMEEG: opensource software for quasistatic bioelectromagnetics. BioMed. Eng. OnLine **9**(1), 45. 2010/09/06 2010. https://doi.org/10.1186/1475-925X-9-45